Available online at www.sciencedirect.com
SCIENCE DIRECT
Polymer 46 (2005) 4891–4898
polymer
www.elsevier.com/locate/polymer

Morphology, thermal, and viscoelastic properties of poly(glycidyl methacrylate-*co*-methyl methacrylate)-based nanocomposites with various organo-modified clays

Yoshihiro Someya, Mitsuhiro Shibata*

Department of Industrial Chemistry, Faculty of Engineering, Chiba Institute of Technology, 2-17-1, Tsudanuma, Narashino, Chiba 275-0016, Japan

Received 11 August 2004; accepted 18 March 2005
Available online 22 April 2005

Abstract

New nanocomposites of poly(glycidyl methacrylate-*co*-methyl methacrylate) (PGM) cured with cyclohexanedicarboxylic anhydride (CDCA) and layered silicates of inorganic content 3 and 5 wt% were prepared by casting the solution of the mixture and subsequent cross-linking at finally 200 °C. Non-modified montmorillonite (MMT) and organo-MMTs (ODA-M, ALA-M, LEA-M, and HBP-M) modified with octadecylamine, 12-aminolauric acid, *N*-lauryldiethanolamine, and hexadecyltributylphosphonium bromide, respectively, were used as layered silicates. X-ray diffraction and morphological studies using transmission electron microscopy revealed that the highly intercalated nanocomposites with the interlayer spacing more than 5.5 nm are formed for the PGM–CDCA/ODA-M, LEA-M, and HBP-M composites with inorganic content 3 wt%. When the inorganic content was increased from 3 to 5 wt%, the degree of intercalation of all the PGM–CDCA/organoclay composites was lowered. Dynamic viscoelastic measurement revealed that the organoclay nanocomposites have significantly higher storage modulus than the PGM–CDCA neat resin. The thermogravimetric analysis revealed that the HBP-M composite with inorganic content 5 wt% has the highest thermal decomposition temperature.

Keywords: Nanocomposites; Poly(glycidyl methacrylate-*co*-methyl methacrylate); Montmorillonite

1. Introduction

In recent years, there has been great attention to polymer/clay nanocomposites, because these materials often exhibit greatly improved mechanical, thermal, barrier, and fire retardant properties at a very low clay content (in general, less than 5 wt%) [1–4]. This is in a marked contrast to conventional reinforcing materials, such as talc, mica, silica, and glass fiber, which require high concentrations and thus incur processing and disposing difficulties, to provide a fraction of these enhancements. The nanocomposites can be prepared by mainly three different methods: in situ intercalative polymerization, polymer melt intercalation, and solution intercalation [5]. Regarding the nanocomposites based on poly(methyl methacrylate) (PMMA), although many literatures have been reported on the in situ intercalative polymerization of methyl methacrylate [6–15], there have been fewer reports on the polymer melt intercalation [16–18] and solution interaction methods [19]. For example, Kumar et al. reported that the melt intercalation method afforded an intercalated nanocomposite which has a higher thermal decomposition temperature (T_d) than pure PMMA [17]. Hwu et al. reported that the intercalated nanocomposite prepared by the solution method shows a higher glass transition temperature (T_g) and a higher T_d [19]. On the other hand, the nanocomposites of acid anhydride-cured epoxy resins can be prepared by essentially in situ intercalative polymerization method [20–27] because the cured polymers are non-fusible and insoluble. For example, Zhang et al. reported that the nanocomposite prepared from diglycidyl ether of bisphenol A and 4-methyl-1,2-cyclohexanedicarboxylic dianhydride shows a higher T_g, T_d and storage modulus than the pure cured epoxy resin [21]. New nanocomposites based on the PMMA copolymers with thermosetting epoxy groups are expected to have superior heat resistance and rigidity. This study describes the

* Corresponding author. Tel.: +81 47 478 0423; fax: +81 478 0439.
E-mail address: shibata@pf.it-chiba.ac.jp (M. Shibata).

0032-3861/$ - see front matter © 2005 Elsevier Ltd. All rights reserved.
doi:10.1016/j.polymer.2005.03.097

preparation and characterization of the new nanocomposites based on the poly(glycidyl methacrylate-*co*-methyl methacrylate) (PGM) cured with cyclohexanedicarboxylic anhydride (CDCA) and various organo-modified clays by the solution intercalation and subsequent in situ polymerization. The objective of our research is to investigate the change of the morphologies accompanied by curing and the influence of the kind of organoclays on the morphologies, thermal and mechanical properties of the PGM–CDCA nanocomposites.

2. Experimental

2.1. Materials

The poly(glycidyl methacrylate-*co*-methyl methacrylate) (PGM) used in this study is BLEMER CP-50M (weight-average molecular weight (M_w): 8200, epoxy equivalent: 297 g/eq., feed weight ratio of glycidyl methacrylate/methyl methacrylate: 50/50) supplied from NOF Corporation (Tokyo, Japan). 1,2-Cyclohexanedicarboxylic anhydride (CDCA) and tetrabutylphosphonium bromide (TBPB) were supplied from New Japan Chemical Co., Ltd (Osaka, Japan) and Hokko Chemical Industry Co., Ltd (Tokyo, Japan), respectively. Sodium montmorillonite (Na^+-MMT, Kunipia F, cation exchange capacity (CEC): 115 meq./100 g) was supplied by Kunimine Industries Co. Ltd (Tokyo, Japan). The surfactants for the preparation of organophilic montmorillonites were octadecylamine (ODA), 12-aminolauric acid (ALA), *N*-lauryldiethanolamine (LEA), and hexadecyltributylphosphonium bromide (HBP) which were supplied from Tokyo Kasei Kogyo Co., Ltd (Tokyo, Japan). Propylene glycol monomethyl ether acetate (PGMEA) was purchased from Wako Pure Chemical Industries, Ltd (Osaka, Japan). All the other chemicals used in this work were reagent grade and used without further purification.

2.2. Preparation of organoclays

Organo-modified MMTs were prepared by cation exchange of natural counterions with organic ammonium and phosphonium compounds. In cases of ODA-M, LEA-M, and ALA-M, molar ratio of exchangeable cation calculated from CEC value, amine, and hydrochloric acid is 1.00:1.50:2.25. A typical procedure in case of LEA is as follows: Na-MMT (10.0 g, exchangeable cation 11.5 mmol) was dispersed in 1000 mL of deionized water at room temperature. LEA (4.73 g, 17.3 mmol) was dissolved in a mixture of deionized water (78 mL) and concentrated hydrochloric acid (2.24 mL, 26.0 mmol) and slowly poured into the clay suspension. The suspension was stirred for 1 h at 80 °C. The exchanged clay was filtered, washed with a 1:1 mixture of water and ethanol, and redispersed in deionized water. This procedure was repeated several times until no chlorine ion was detected with 0.14 N $AgNO_3$ solution. The filter cake was freeze-dried, crushed into powder using mortar and pestle, and screened with a 280-mesh sieve. The LEA-modified MMT is denoted as LEA-M. HBP-M was also prepared in a similar manner except for no use of hydrochloric acid.

The cation exchange rates of ALA-M, ODA-M, LEA-M, and HBP-M were 74.2, 91.2, 68.9, and 95.2%, respectively. Their organic fractions were 15.8, 22.5, 18.1, and 32.5 wt%, respectively.

2.3. Preparation of composites

The clays (Na-MMT, organo-MMTs) were dried under vacuum at 40 °C for at least 24 h before use. To a solution of PGM (10.0 g, epoxy group: 33.7 mmol) and PGMEA (90 g), were added CDCA (5.20 g, 33.7 mmol) and TBPB (50 mg). After the solution was stirred for 24 h, clay was added and stirred for 24 h at room temperature. The resulting suspension was cast on a poly(tetrafluoroethylene-*co*-perfluoroalkyl vinyl ether) (PFA)-coated stainless steel plate, dried at 70 °C for 24 h and further at 100 °C for 24 h, and cured at 140 °C for 3 h, at 180 °C for 2 h, and finally at 200 °C for 2 h to give a cured PGM–CDCA/clay film. The PGM/clay films without CDCA were also prepared by casting a solution of PGM and clay, and subsequent drying at 60 °C for 24 h and further at 100 °C for 24 h.

2.4. Measurements

Cation exchange rate (CER) of organoclay was calculated from cation exchange capacity (CEC: 115 meq./100 g) of Kunipia F, and the weight decrease [W_1(g)] and remaining weight [W_2(g)] measured by thermogravimetric analysis (TGA) on a Perkin Elmer TGA-7 instrument when the organoclay was heated from room temperature to 700 °C with a heating rate of 20 °C/min in a nitrogen atmosphere. CER is calcultated from the following equation: $\mathrm{CER}(\%) = 100(W_1/M_w)/[10^{-5}\mathrm{CEC}(W_2 + 23.0W_1/M_w)]$ where M_w is the molecular weight of organic ammonium cation. Organic fraction (wt%) of organoclay is $100W_1/(W_1 + W_2)$.

X-ray diffraction (XRD) analysis was performed at ambient temperature on a Rigaku RINT-2100 X-ray diffractometer at a scanning rate of 2.0°/min, using Cu K_α radiation (wavelength, $\lambda = 0.154$ nm) at 40 kV and 14 mA. Sodium montmorillonite and the organoclays were studied as powders. The post-cured composites of ca. 1 mm thickness were used for the XRD measurement.

Dynamic viscoelastic measurements of the films were performed on a Rheolograph Solid (Toyo Seiki Co., Ltd, Japan) with a chuck distance of 20 mm, a frequency of 10 Hz and a heating rate of 2 °C/min. Transmission electron microscopy (TEM) was performed on an electron microscope with a 75 kV accelerating voltage. The dumbbell-shaped samples were sectioned into roughly 100 nm thin sections at room temperature using an ultramicrotome with

a diamond knife and then mounted on 200 mesh copper grids.

The 5% weight loss temperature was measured on a Perkin Elmer thermogravimetric (TG) analyzer TGA 7 in a nitrogen atmosphere at a heating rate of 20 °C/min.

3. Results and discussion

3.1. Dispersion of clays in the PGM and cured PGM composites

The extent of intercalation and exfoliation of the PGM/clay and cross-linked PGM–CDCA/clay composites were evaluated by means of XRD measurements. Fig. 1 shows XRD patterns of clays, and the PGM/clay and PGM–CDCA/clay composites with inorganic content 3 wt%. Table 1 summarizes the interlayer spacing of the clays and composites. The strongest peaks correspond to the [001] basal reflection of the silicate layers. From the angular location of the peaks and the Bragg condition the interlayer spacing (d_1) of each of the clays was determined. The interlayer spacing of the clays increased with the order of MMT ≪ ALA-M < LEA-M < ODA-M < HBP-M. The surfactant having bulkier substituent on the nitrogen or phosphorus atom shows a higher interlayer spacing. When the interlayer spacing (d_2) of PGM/clay composite with inorganic content 3 wt% was compared to that of the corresponding clay itself (d_1), all the PGM/organoclay composites (0.8–2.1 nm) showed a higher d_2–d_1 value than the PGM/MMT composite (0.40 nm), indicating that the intercalated nanocomposites are formed for the former composites. Regarding a little enlargement for the unmodified MMT composite, it is thought that the solvent PGMEA or the impurities contained in PGM intercalated into the MMT because PGM itself should be hard to intercalate in the unmodified MMT. The XRD analysis of the MMT stirred for 24 h in PGMEA revealed that no intercalation of PGMEA occurs. The GPC and ^{1}H NMR analyses of the PGM used in this study suggested that the PGM contains ca. 7% low molecular weight component with M_w 630 (polystyrene standard) and that a multiple proton signal probably related to alcoholic hydroxyl group is observed at 4.4 ppm. Although we could not assign the

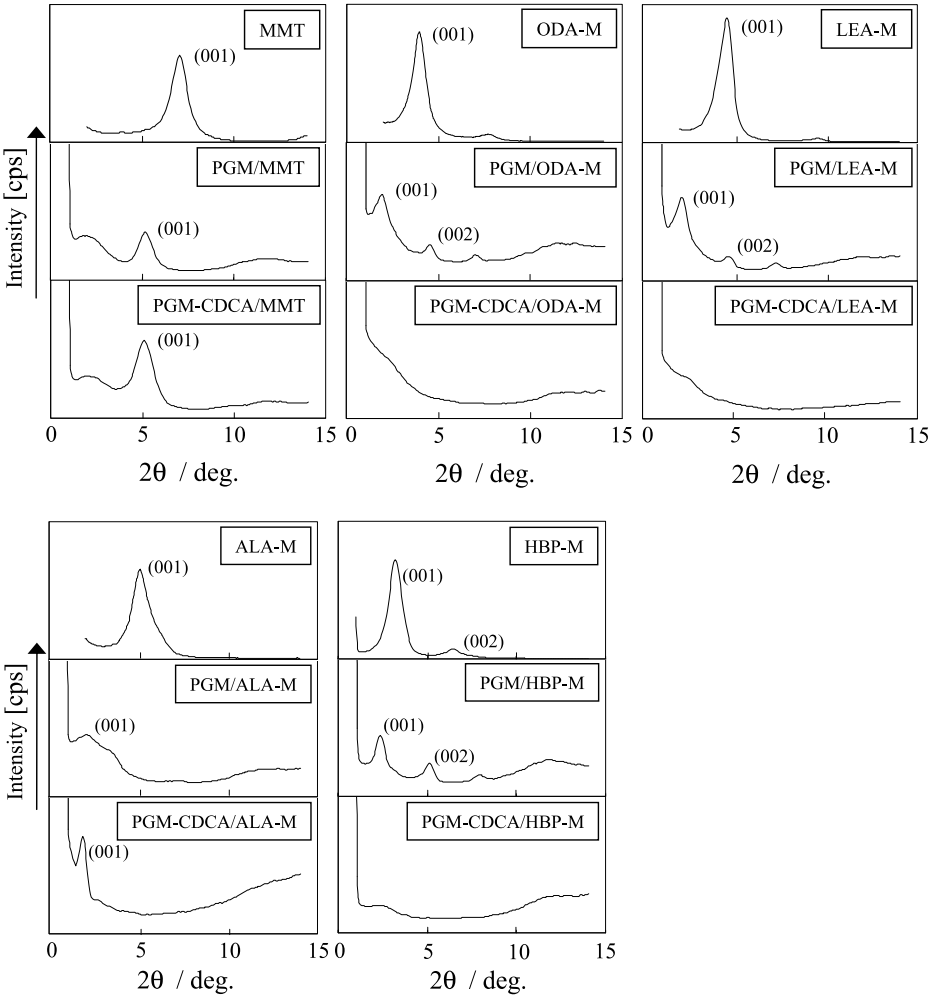

Fig. 1. XRD patterns of clays, and the PGM/clay and PGM–CDCA/clay composites with inorganic content 3 wt%.

Table 1
Interlayer spacing as determined by XRD analysis for clays and the composites with inorganic content 3 wt%

Clay	XRD peak position (2θ)			Interlayer spacing [001] (nm)		
	In clay	In composite		In clay (d_1)	In composite (d_2)	
		PGM	PGM–CDCA		PGM	PGM–CDCA
MMT	7.02	5.32	5.42	1.26	1.66	1.63
ODA-M	4.04	2.18	–	2.19	4.05	–
LEA-M	4.88	2.38	–	1.81	3.71	–
ALA-M	5.16	2.32	2.12	1.71	3.80	4.16
HBP-M	3.40	2.60	–	2.60	3.40	–

clear structure of the impurities of the PGM, the hydroxyl compound may intercalate into MMT. For PGM/ALA-M composites, the main peak at 2.32° (3.80 nm) contained a broad shoulder peak around 1.3–4.0°, suggesting that some of the epoxy groups of the intercalated PGM may react with the carboxylic acid group of ALA.

Next, regarding the cross-linked composites, the PGM–CDCA/MMT composite showed almost the same XRD pattern as PGM/MMT composite, indicating that no intercalation occurs. On the other hand, the peak related to the intercalation observed for the PGM/clay composites without CDCA disappeared for PGM–CDCA/ODA-M, LEA-M, and HBP-M composites. If the peak shifts to a 2θ region less than 1.6°, that is corresponding to interlayer spacing 5.5 nm, the peak cannot be observed because of overlapping with a steep base line. Therefore, the presence of ordered layer structure at a higher interlayer spacing (> 5.5 nm) could not be confirmed from the XRD data. TEM allows the morphological state of the nanocomposite to be delineated more completely. In case of PGM–CDCA/ALA-M composite, although most of the broad peak observed for PGM/ALA-M at 1.3–4.0° disappeared and a sharp peak was still observed at 2.12° (4.16 nm), suggesting the presence of intercalated silicate layers. We suppose that the intercalated polymers ionically cross-linked between the two adjacent clay layers are generated by the reaction of the carboxylic acid groups bearing on the surface of ALA-M with the epoxy groups of PGM, which disturb the exfoliation of the clay layers. A similar mechanism had been already reported in our previous paper [28].

Fig. 2 shows the XRD patterns of PGM–CDCA/ODA-M, LEA-M, ALA-M, and HBP-M composites with inorganic content 5 wt%. Although no clear XRD peak was observed for the PGM–CDCA/ODA-M, LEA-M and HBP-M composites with inorganic content 3 wt%, the 5 wt% composites showed the peaks corresponding to the [001] basal reflection of the silicate layers. The HBP-M 5 wt% composite showed the peak at 3.20° (2.76 nm), which is near to the peak (3.40°, 2.60 nm) of HBP-M itself, suggesting the presence of the non-intercalated clay. The ODA-M 5 wt% composite showed the peak at 1.70° (5.19 nm), which is much higher interlayer spacing than ODA-M itself (2.19 nm), indicating the presence of still highly intercalated nanocomposite. The ALA-M 5 wt% composite (3.18 nm) showed a lower interlayer spacing than the ALA-M 3 wt% composite (4.16 nm). The increase of clay content caused a lowering of the degree of intercalation in all cases. Among the 5 wt% composites, the ODA-M composite had the largest interlayer spacing.

Fig. 3 shows TEM image of the PGM–CDCA/clay composites with inorganic content 3 wt%. It is obvious that the PGM–CDCA/ODA-M composite has a much better and finer dispersion of clays than the PGM–CDCA/MMT composite composed of micro-scale clusters or agglomerated particles (Fig. 3(a) and (b)). Although the XRD peak corresponding to the interlayer spacing was not observed for

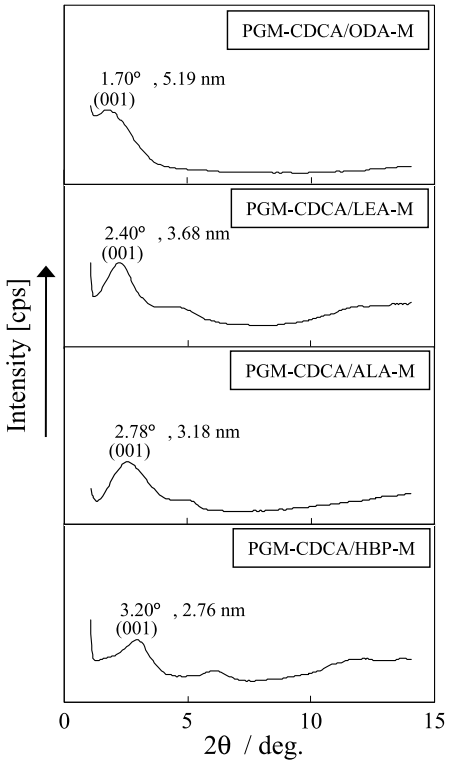

Fig. 2. XRD patterns of the PGM–CDCA/organoclay composites with inorganic content 5 wt%.

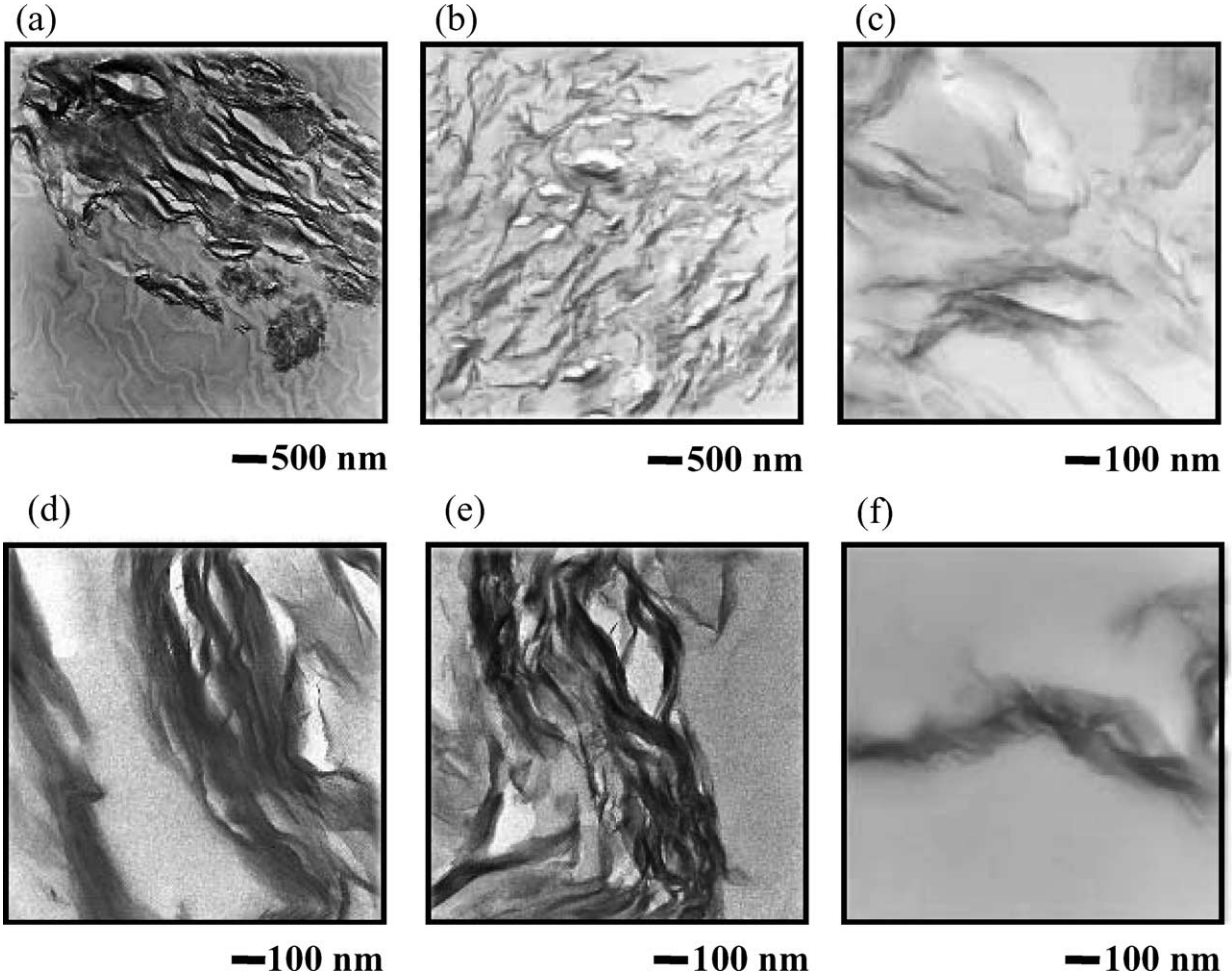

Fig. 3. TEM images of the PGM–CDCA/clay composites with inorganic content 3 wt%: (a)PGM–CDCA/MMT, (b) and (c) PGM–CDCA/ODA-M, (d) PGM–CDCA/LEA-M, (e) PGM–CDCA/ALA-M, (f) PGM–CDCA/HBP-M.

the PGM–CDCA/ODA-M, LEA-M, and HBP-M composites with inorganic content 3 wt%, none of the composites become a completely exfoliated nanocomposite (Fig. 3(c), (d) and (f)). All the PGM–CDCA/organoclay composites appear to be intercalated nanocomposites where the interlayer order is considerably retained. It appeared that the PGM–CDCA/ODA-M and PGM–CDCA/HBP-M composites have less agglomerated clusters than the other composites.

3.2. Mechanical and thermal properties of the PGM composites

Fig. 4 shows the temperature dependence of storage modulus (E') of the PGM composites with inorganic content 3 wt%. The storage moduli of glassy state (<ca. 50 °C) and rubbery state (>ca. 150 °C) of the intercalated PGM–CDCA nanocomposites were considerably higher than those of the PGM–CDCA resin. Especially, the improvement at the rubbery plateau was higher. Above T_g, when materials become soft, the reinforcement effect of the clay particles becomes prominent, due to restricted movement of the

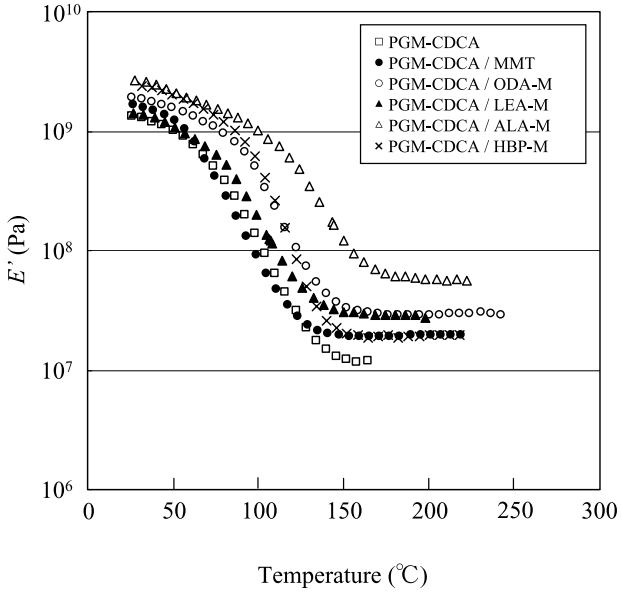

Fig. 4. Temperature dependence of the storage modulus (E') of the PGM–CDCA/clay composites with inorganic content 3 wt%.

polymer chains, and hence strong enhancement of modulus appears. Although the PGM/ALA-M composite has a less degree of intercalation and the dispersion of clay is not so good, the ALA-M composite showed the highest storage modulus among all the composites. Table 2 summarized the tan δ peak temperature which corresponds to T_g. The order of higher tan δ peak temperature of the clay composites with inorganic content 3 wt% was ALA-M $\gg$ HBP-M > ODA-M > LEA-M > MMT. In order to clarify the reason for a high T_g and storage modulus of the ALA-M composite, the dynamic viscoelastic measurement of the PGM resin cured with CDCA in the presence of ALA corresponding to inorganic content 3 wt% was examined. The PGM–CDCA–ALA resin without clay showed a higher T_g (117.9 °C) and storage modulus (1.41 GPa at 50 °C) than PGM–CDCA resin (109.9 °C, 1.02 GPa). This result suggests that the carboxylic acid group of ALA reacts with the epoxy group of PGM, and/or catalytically promotes the curing reaction between PGM and CDCA. A similar trend has been quite recently reported for the nanocomposite based on the montmorillonite modified with terminal carboxylic acid group-containing cocamidopropylbetaine and bisphenol A epoxy resin cured with methyl tetrahydrophthalic anhydride [20]. When the inorganic content was increased from 3 to 5 wt%, the storage modulus and tan δ peak temperature of the ODA-M and LEA-M composites considerably rose, while those of the ALA-M and HBP-M composites rather decreased. (Fig. 5) This result is in agreement with the morphological change between the 3 and 5 wt% composites evaluated by XRD analyses.

Fig. 6 shows TGA curves of the PGM–CDCA resin and the PGM–CDCA/clay composites with inorganic content 3 wt% in a nitrogen atmosphere. The PGM–CDCA/HBP-M composite has the highest 5 wt% weight loss temperature (T_d: 284.7 °C) in the organoclay composites with inorganic content 3 wt%. This trend is much remarkable when the inorganic content is 5 wt% (PGM–CDCA/HBP-M: 308.5 °C), as is shown in Table 2. The heat resistance of the clay composites may be associated with complex factors such as the action of clay as a free-radical scavenger, the decomposition of organic modifier, and the gas barrier properties due to clay dispersion. Regarding the decomposition of organic modifier, HBP-M has a superior thermal stability among the organoclays used in this study, as is obvious from the TGA curves of clays themselves shown in Fig. 7. The highest decomposition temperature of the HBP-M composite should be associated with a higher thermal stability of the alkylphosphonium in addition to the improved gas barrier properties due to the formation of nanocomposite [29]. Also, a higher decomposition temperature of the MMT composite than the neat resin may be related to the deactivation of thermally generated radical species on the Lewis acid surface of the aluminosilicate (Fig. 7 and Table 2) [30]. In case of the composites using ammonium-treated clays, the decomposition of the polymer in the composites is thought to be initiated by the decomposition of the ammonium-type organo-modifier on the clay surface. The PGM–CDCA/ODA-M composite with inorganic content 5 wt% showed considerably higher T_d than the ODA-M 3 wt% composite (Table 2). This result may be associated to the increase of the exfoliated/intercalated aluminosilicates and the highest decomposition temperature of ODA-M among the organoammonium-type MMT. As is obvious from Fig. 7, LEA-M itself showed a two-step thermal decomposition which may be related to the bis(hydroxyethyl) and lauryl groups. Corresponding to this result, the LEA-M composite with inorganic content 5 wt% showed a lower T_d than the HBP-M and ODA-M composites with inorganic content 5 wt%. Although the decomposition temperature of ALA-M itself is not so low, the ALA-M composite with inorganic content 5 wt% showed the lowest decomposition temperature (245.1 °C). This may be related to the difference of curing mechanism from the case using other organo-modifier due to the action of the carboxylic acid group, and also the lowering of the clay dispersion with increasing amount of ALA-M.

Table 2
Thermal properties of PGM–CDCA/clay composites and clays

Sample	Inorganic content (wt%)	Tan δ peak temperature (°C)	5% weight loss temperature (°C)
PGM–CDCA	0.0	109.9	277.2
PGM–CDCA/MMT	3.0	93.0	286.3
PGM–CDCA/ODA-M	3.0	116.0	277.4
PGM–CDCA/ODA-M	5.0	153.0	283.1
PGM–CDCA/LEA-M	3.0	108.0	282.2
PGM–CDCA/LEA-M	5.0	130.0	270.6
PGM–CDCA/ALA-M	3.0	144.1	275.8
PGM–CDCA/ALA-M	5.0	139.2	245.1
PGM–CDCA/HBP-M	3.0	122.0	284.7
PGM–CDCA/HBP-M	5.0	116.9	308.5
ODA-M	–	–	352.8
LEA-M	–	–	270.5
ALA-M	–	–	301.9
HBP-M	–	–	332.8

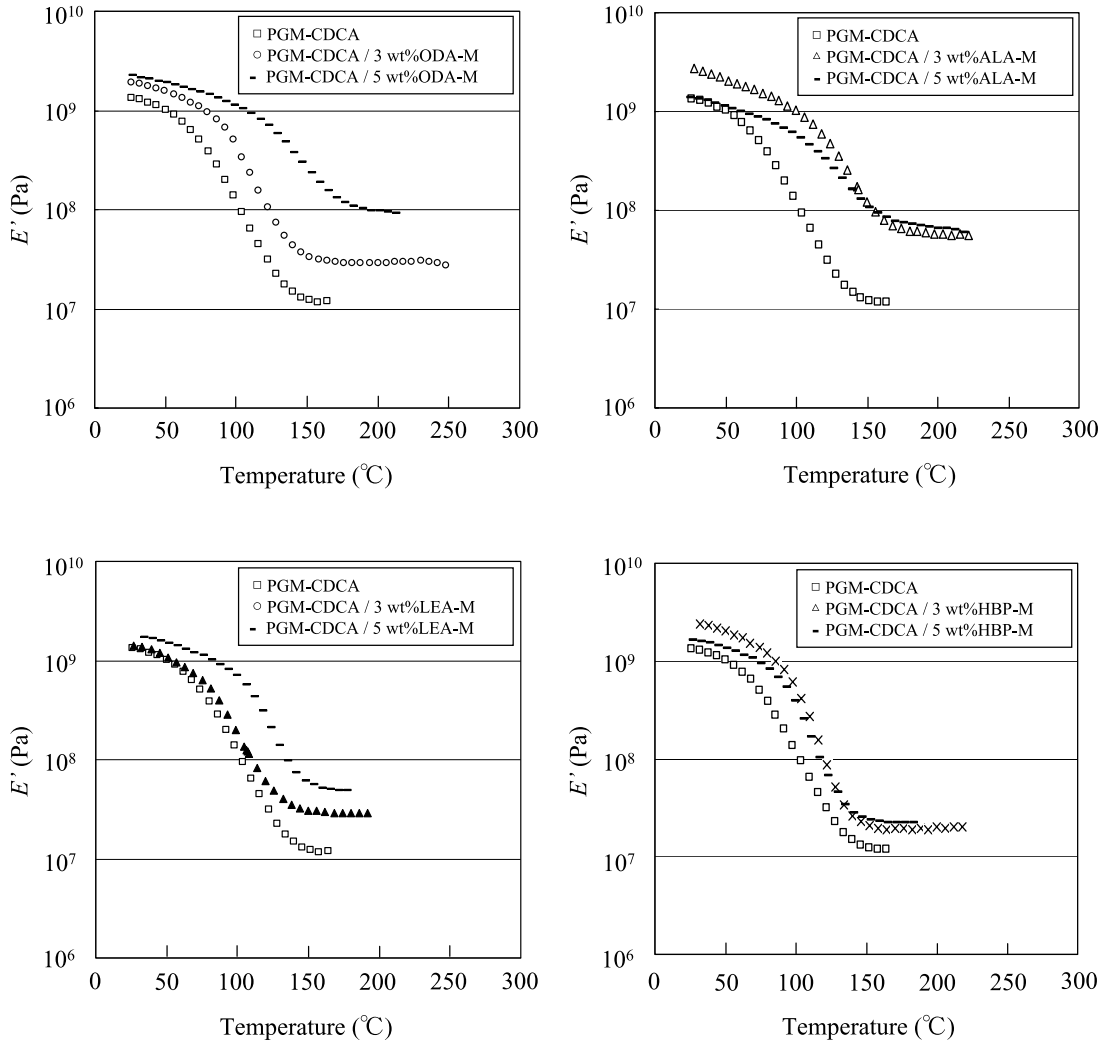

Fig. 5. Comparison of E' of the PGM–CDCA/organoclay composites with inorganic content 3 and 5 wt%.

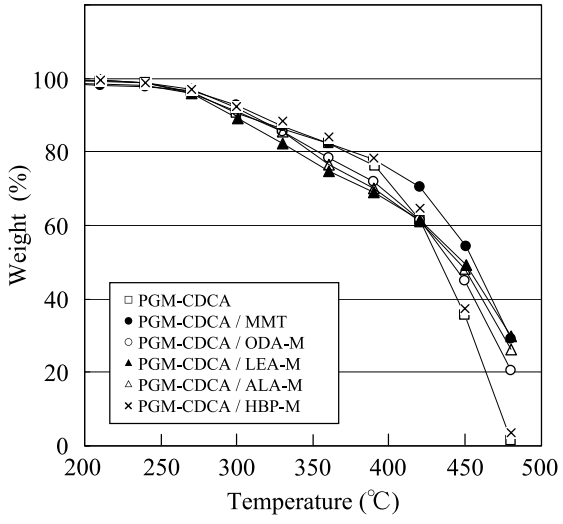

Fig. 6. TGA curves of the PGM–CDCA/clay composites with inorganic content 3 wt%.

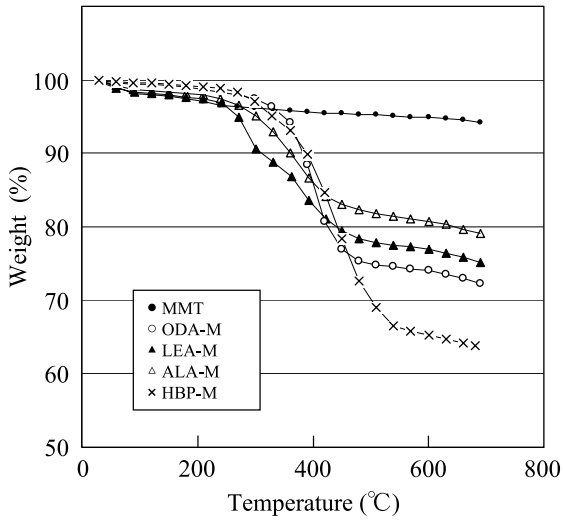

Fig. 7. TGA curves of various clays.

4. Conclusions

The nanocomposites of PGM and PGM–CDCA with MMT, ODA-M, LEA-M, ALA-M, HBP-M of inorganic content 3 and 5 wt% were prepared by casting the solution of the mixture and subsequent cross-linking at finally 200 °C. The XRD and TEM analyses revealed that the highly intercalated nanocomposites with the interlayer spacing more than 5.5 nm are formed for the PGM–CDCA/ODA-M, LEA-M, and HBP-M composites with inorganic content 3 wt%, although complete exfoliation does not occur. The intercalated nanocomposite with the interlayer spacing of 4.16 nm was formed for the PGM–CDCA/ALA-M composite with inorganic content 3 wt%. When the inorganic content was increased from 3 to 5 wt%, the degree of intercalation of all the composites using organoclays was lowered. Dynamic viscoelastic measurement revealed that the PGM–CDCA nanocomposites have significantly higher E' and T_g than the PGM–CDCA neat resin. In case of highly intercalated PGM–CDCA/ODA-M and LEA-M composites, the increase of inorganic content resulted in a further increase of E' and T_g. The TGA revealed that the HBP-M composite with inorganic content 5 wt% shows the highest T_d. Although the PGM–CDCA/ODA-M composite with inorganic content 5 wt% showed a higher T_d than the ODA-M 3 wt% composite, the T_d of the ALA-M composite was rather lowered by the increase of the clay.

Acknowledgements

The authors wish to thank Mr Yoshifumi Yoshida and Mr Shigeki Naitoh, IT-Related Chemicals Research Laboratory, Sumitomo Chemical Co., Ltd, Japan for financial supports and helpful suggestions, and also would like to thank Mr Jun Ikeda and Mr Tetsu Asano, IT-Related Chemicals Research Laboratory, Sumitomo Chemical Co., Ltd, Japan for taking TEM pictures.

References

[1] Usuki A, Kojima Y, Kawasumi M, Okada A, Fukushima Y, Kurauchi T, et al. J Mater Res 1993;8(5):1179–84.
[2] Yano K, Usuki A, Kurauchi T, Kamigaito O. J Polym Sci, Part A: Polym Chem 1993;31(10):2493–8.
[3] Messersmith PB, Giannelis EP. Chem Mater 1994;6(10):1719–25.
[4] Messersmith PB, Giannelis EP. J Polym Sci, Part A: Polym Chem 1995;33(7):1047–57.
[5] Alexandre M, Dubois P. Mater Sci Eng R 2000;R28:65P.
[6] Meneghetti P, Qutubuddin S. Langmuir 2004;20(8):3424–30.
[7] Wilkie CA, Jiang DD, Su S. Polym Adv Technol 2004;15(5):225–31.
[8] Xu Y, Brittain WJ, Xue C, Eby RK. Polymer 2004;45(11):3735–46.
[9] Li Y, Zhao B, Xie S, Zhang S. Polym Int 2003;52(6):892–8.
[10] Xie T, Yang G, Fang X, Ou Y. J Appl Polym Sci 2003;89:2256–60.
[11] Zhu J, Start P, Mauritz KA, Wilkie CA. Polym Degrad Stab 2002; 77(2):253–8.
[12] Huang X, Brittain WJ. Macromolecules 2001;34(10):3255–60.
[13] Okamoto M, Morita S, Kim YH, Kotaka T, Tateyama H. Polymer 2001;42(3):1201–6.
[14] Okamoto M, Morita S, Taguchi H, Kim YH, Kotaka T, Tateyama H. Polymer 2000;41(10):3887–90.
[15] Lee DC, Jang LW. J Appl Polym Sci 1996;61(7):1117–22.
[16] Shen Z, Simon GP, Cheng YB. J Appl Polym Sci 2004;92(4): 2101–15.
[17] Kumar S, Jog JP, Natarajan U. J Appl Polym Sci 2003;89(5):1186–94.
[18] Gelfer MY, Song HH, Liu L, Hsiao B, Chu B, Rafailovich M, et al. J Polym Sci, Part B: Polym Phys 2003;41(1):44–54.
[19] Hwu JM, Jiang GJ, Gao ZM, Xie W, Pan WP. J Appl Polym Sci 2002; 83:1702–10.
[20] Guo B, Ouyang X, Cai C, Jia D. J Polym Sci, Part B: Polym Phys 2004;42(7):1192–8.
[21] Zhang K, Wang L, Wang G, Li Z. J Appl Polym Sci 2004;91(4): 2649–52.
[22] Torre L, Frulloni E, Kenny JM, Manferti C, Camino G. J Appl Polym Sci 2003;90(9):2532–9.
[23] Lue J, Ke Y, Qi Z, Yi X. J Polym Sci, Part B: Polym Phys 2001;39(1): 115–20.
[24] Zilg C, Muelhaupt R, Thomann R. Polym Mater Sci Eng 2000;82: 249–50.
[25] Zilg C, Thomann R, Muelhaupt R, Finter J. Macromol Mater Eng 2000;280/281:41–6.
[26] Ke Y, Zhao J, Gi Z, Lue J, Yi X. J Appl Polym Sci 2000;78(4): 808–15.
[27] Zilg C, Muelhaupt R, Finter J. Macromol Chem Phys 1999;200(3): 661–70.
[28] Someya Y, Shibata M. Polym Eng Sci 2004;44(11):2041–6.
[29] Kim MH, Park CI, Choi WM, Lee JW, Lim JG, Park OO, et al. J Appl Polym Sci 2004;92(4):2144–50.
[30] Huang X, Brittain WJ. Macromolecules 2001;34:3255–60.